Journal of the European Ceramic Society **19** (1999) 17–31

PII: S0955-2219(98)00158-7
0955-2219/98/$—see front matter

Mechanical and Microstructural Change in 0–90° SiC/MAS-L Composites after Thermal Ageing: Vacuum, Ar and CO Atmosphere

Christine Labrugère,* Laurent Guillaumat, Alain Guette and Roger Naslain

Laboratoire des composites thermostructuraux, (UMR-47,CNRS-SEP-UB1), 3 allée de la Boëtie, 33600 Pessac, France

(Received 6 February 1998; accepted 16 June 1998)

Abstract

To determine the effects of an oxidizing environment on SiC (ex-PCS) fibres, 0–90° cross-plyed (2D) SiC/MAS-L composites have been heat-treated under vacuum, argon and CO in the 900–1200°C temperature range. The mechanical behaviour of the material was assessed by room temperature tensile tests and correlated to the fibre, matrix and interfacial zone changes. Transmission electron microscopy (TEM), Auger electron spectroscopy (AES) and electron probe microanalysis (EPMA) were used to characterize the fibre and fibre/matrix interface. The degree of crystallization of the matrix was obtained using X-ray diffraction (XRD). The fibre/matrix bond strength is characterized by push-out tests on thin slices. Up to 1000°C under vacuum, the material was quite stable with a better fibre/matrix bond strength leading to an increase in the composite ultimate tensile strength. As soon as the temperature was raised to near 1100°C, the crystallization of the matrix, largely influenced by the atmosphere nature, resulted in a drop in the mechanical properties of the composite. The fibre/matrix interfacial zone as well as the fibres were modified by insitu *phenomena such as diffusion of Si, Al or Mg species coming from the matrix, or by reaction with the CO atmosphere. © 1998 Elsevier Science Limited. All rights reserved*

Resumé

Afin de déterminer l'influence d'un environnement oxydant sur les fibres SiC (ex-PCS), des composites SiC/MAS-L à empilement de plis croisés 0–90° ont été vieillis sous vide, sous argon ou sous CO dans une gamme de température comprise entre 900 et 1200°C. Le comportement mécanique du matériau est suivi par des essais de traction à l'ambiante et corrélé à l'évolution de la fibre, de la matrice et de la zone interfaciale. La microscopie électronique en transmission (TEM), la spectroscopie d'électrons Auger (AES) ainsi que la microsonde électronique à spectrométrie de rayons X (EPMA) constituent les principaux moyens de caractérisation chimique et microstructurale de la fibre et de la zone interfaciale fibre/matrice. L'état de cristallisation de la matrice est déterminé par diffraction de rayons X (XRD). De plus, la liaison fibre/matrice est évaluée par des essais de push-out sur lames minces. Jusqu'à 1000°C sous vide, le matériau reste stable avec un renforcement de la liaison fibre/matrice conduisant à une augmentation de la contrainte à rupture du composite. Dès que la température avoisine 1100°C, la cristallisation de la matrice, très nettement influencée par la nature de l'atmosphère de vieillissement, entraîne une chute des propriétés mécaniques du composite. La zone interfaciale fibre/matrice de même que les fibres évoluent suite à des réactions internes au matériau avec diffusion des éléments Si, Al ou Mg provenant de la matrice, ou bien après réaction avec l'atmosphère de CO.

Keywords: Sic composites, fibres, B. interfaces, ageing

1 Introduction

Glass-ceramic matrix composites reinforced with continuous ceramic fibres offer interesting future prospects for thermostructural applications below 1000°C. Materials such as SiC (Nicalon or Tyranno) fibres/glass-ceramic matrix composites have been developed because they exhibit a non brittle behaviour after elaboration process due to weak fibre/matrix bonding (i.e. interfacial carbon thin layer growing during the process).[1–8] Fibres in the as-received composites can also be partially

*To whom correspondence should be addressed. Fax: +33-055-684-2761; e-mail; labruger@icmcb.u.-bordeaux.fr

debonded from the matrix on account of their thermal expansion mismatch. Therefore, interfacial shear stress values currently measured by micro-indentation (push-out) are particularly low ($\tau <$ 5 MPa).[9–14]

Since development of these materials is relatively new,[15,16] the influence of heat-treatments up to 1100°C (maximum operating temperature) on the constituents of the composite have not been completely studied. Previous investigations have been made in air, revealing that even limited exposures at elevated temperatures decreased the utility of such composites after the carbon layer was substituted by silica (e.g. reinforcement of the fibre/matrix bonding and loss of the mechanical properties).[1,2,12,17,18]

Consequently, other types of ageing atmospheres have been considered in the present work to vary the properties of SiC/glass-ceramic composites. Thus SiC/MAS-L composites (made and furnished by Aerospatiale) were aged between 900 and 1200°C under vacuum, argon or a CO atmosphere. The objective was to understand the Nicalon SiC fibre thermal change when the fibers are in an oxidizing lithium–magnesium–aluminosilicated matrix, also to understand the fibre/matrix (FM) interfacial zone change.

2 Experimental

2.1 Materials

The materials used in the present investigation are SiC/MAS-L composites formed by a stack of twelve unidirectional sheets of Si–C–O (ex-PCS) fibres (NLM 202 fibres from Nippon Carbon), previously infiltrated, 0–90° cross-plyed (0–90° 2,s) and pressed together at high temperature (i.e. $T \approx 1300$°C) under nitrogen. The residual porosity of the composite is very low, approximately 1%. The fibre volume fraction (*Vf*) is of about 40%. The matrix is obtained from a vitreous powder which is synthesized from organometallic precursors according to the sol-gel process.[15,16] The corresponding chemical composition is: 0·5 MgO-0·5 Li_2O-1 Al_2O_3-4SiO_2.

Mechanical characteristics of the as-received SiC/MAS-L composite are a stress to rupture at room temperature equal to 170 MPa with a strain of 0·4% and a Young's Modulus of about 95 GPa. Once the tensile fracture, the length of pulled-out fibres can reach several millimetres (Fig. 1) giving evidence of a low interfacial shear stress estimated between 2 and 5 MPa.[12–14] Rectangular samples ($100 \times 10 \times 3\,mm^3$) were cut with a diamond saw in the composite plates and then shaped for the ageing treatments and the mechanical tensile tests. The external ply is a 90°-orientated sheet.

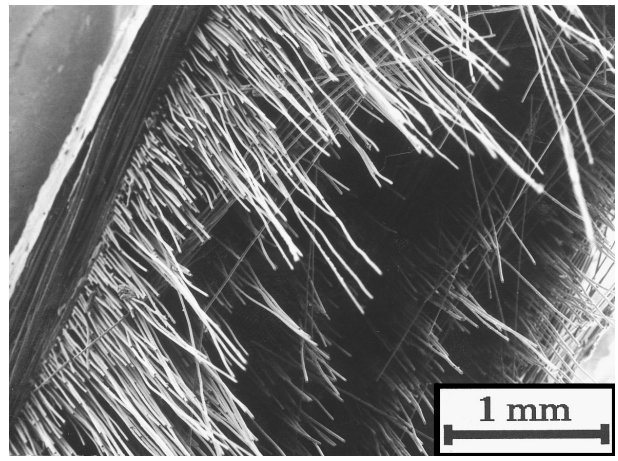

Fig. 1. SEM micrograph of the fractured surface of an as-received 0–90° SiC/MAS-L tensile test specimen: pronounced fibre pull-out.

2.2 Ageing treatments

The ageing treatments have been performed directly on the tensile specimens. The sample (initial weight $m_0 = 7{\cdot}5$ g) was hung to a microbalance (D101 from Cahn, USA) (sensitivity: 0·1 μg) in order to record continuously the weight loss $\Delta m/m_0$, and heated with a graphite susceptor submitted to an induced r.f. current to reach high temperatures in a short time (i.e. 1200°C within less than 15 min). For the treatments under vacuum, the ageing chamber was evacuated with a turbo-molecular pump (residual pressure: 10^{-1}–10^{-3} Pa) whereas those in argon or CO were conducted at constant volume (respectively 70 and 100 kPa). The ageing conditions are listed in Table 1.

2.3 Characterization

The analysis of the FM interfacial zone (in terms of chemical composition and microstructure) has been obtained by transmission electron microscopy (TEM, 2000 FX Jeol, Japan) and by Auger electron spectroscopy (AES, PHI-590 Perkin–Elmer). The samples used for the TEM characterization

Table 1. Ageing conditions applied to 0–90° SiC/MAS-L composite tensile test specimens under vacuum, argon or CO. Weight losses and tensile test results at room temperature

Ageing atmosphere (pressure Pa)	*Ageing T (°C)*	*Ageing time (h)*	$\Delta m/m_o$ *(%)*	σ_r (MPa)	ε_r (%)	*E (GPa)*
As-received	0	0	0	171	0·42	93
Vacuum ($1{\cdot}10^{-3}$)	900	98	−0·2	192	0·63	87
Vacuum ($5{\cdot}10^{-4}$)	1000	96	−0·9	197	0·48	75
Vacuum ($5{\cdot}10^{-3}$)	1100	16	−3	94	0·48	59
Vacuum ($1{\cdot}10^{-4}$)	1100	45	−11·6	32	0·18	35
Vacuum ($1{\cdot}10^{-4}$)	1100	102	−18·7	36	0·17	–
Vacuum ($2{\cdot}10^{-2}$)	1200	1	−18	Weak	–	–
Argon ($7{\cdot}10^{4}$)	1100	19	−2·5	–	–	–
CO ($1{\cdot}10^{5}$)	1100	30	+0·2	131	0·33	83
CO ($1{\cdot}10^{5}$)	1100	96	+0·2/−0·2	72	0·16	86

were cut with a diamond wire saw from aged specimens submitted to tensile test, at a distance of about 15 μm from the failure surface. The specimens were thinned according to a procedure classical for this kind of materials (i.e. mechanically down to 80–150 μm and then etched with Ar^+ ions). The AES analyses were performed according to the depth profiling mode (Ar^+ ion etching) from the surface of pulled-out fibres present at the failure surface of tensile test specimens. The Auger electron transitions which have been used are Si_{LVV} (referred to as Si1) for silicon, C_{KLL} (referred to as C1) for carbon, O_{KLL} (referred to as O1) for oxygen, Al_{LVV} (referred to as Al1) for aluminium and Mg_{LVV} (referred to as Mg1) for magnesium. The apparent atomic concentrations were calculated from the peak to peak heights of the spectra recorded in the derivative dN(E)/dE mode. The elemental composition of the fibre (in the bulk and very near the FM interfacial zone) was assessed by EPMA (Camebax, Cameca France) characterization performed on one polished face of aged specimens. Carbon, oxygen, aluminium and magnesium were analyzed with a wavelength dispersion spectrometer (WDS) (i.e. K(WDS) line for each of them), and silicon with an energy dispersion spectrometer (EDS, Si-Kα peak). These results will be shown as radial concentration profiles. Lithium couldn't be proportioned by EPMA but was qualitatively detected by PEELS (analyzer Gatan coupled to a 300 kV TEM Philips) analyses on thin foils. The matrix constitution was determined by X-ray diffraction (XRD) (D5000 diffractometer Siemens) on a powder of pounded composite with some added silicon powder acting as standard for X-ray lines identification (Si main lines at $d_{hkl} = 0{\cdot}3146$, 0·1920, 0·1638, 0·1357, 0·1246 and 0·1108 nm). The emission anticathode is made of filtered copper (i.e. $\lambda = 0{\cdot}15406$ nm).

The aged samples were tested at room temperature under tensile loading (8501 Instron) at a constant strain rate of 0·05% per min. The evolution of the FM interfacial bonding was assessed qualitatively through indentation push-out tests conducted on specimens of about 300 μm in thickness. The load was applied on the fibres with a Vickers indentor (licensed from Onera France) at a rate of the order of 0·12 μm s^{-1} and measured with a 2 N load cell. The displacement was measured with a capacitive sensor.

3 Results

3.1 As-received composites

The chemical composition of the fibres in the as-received composite is (in at%): Si(37), C(47), O(16) based on EPMA microanalyses. The average size of the SiC-crystals in the fibres (as-derived from the TEM images) is 3 nm and the free carbon is composed of basic structural units (BSU)* as in the fibre before elaboration. A very slight diffusion of Al and Mg from the matrix inside the fibre is usually recorded[19] (i.e. quantities $\leq$ 0·1 at%) as well as a small amount of lithium detected by PEELS.

The FM interface changed during processing forming a carbon layer 20 nm thick between the fibre and the matrix (Figs. 2 and 3). The carbon consists of short aromatic layers stacked in a turbostratic disorder with a thin border of layers parallel to the interface, on the matrix side, over 3–4 nm. Interfacial decohesions usually take place in this well-organized border as-observed by TEM in our samples and previously mentioned by other authors.[19,20] These decohesions can be explained by weak bondings between the aromatic layers or by residual stresses at the FM interface due to different thermal expansion coefficients between the fibre and the matrix (i.e. $\alpha_f \approx 3{\cdot}4\,10^{-6}$ K^{-1} [21] $\alpha_m = 0{\cdot}9$–$1{\cdot}7\ 10^{-6}$ K^{-1} [2]). This phenomenon was assessed by the optical observation of a tensile tested material showing a very large cracking (i.e. 15 μm) (Fig. 4) Fibre surface close to the interfacial carbon layer exhibits a higher oxygen concentration than in the bulk, over 100–150 nm (Fig. 2), as previously described by Grenier[22] in SiC/LAS composites. XRD pattern of the matrix shows a mixture of phases which are (in order of decreasing importance): β-spodumene ($LiAlSi_2O_6$); a 'high quartz' structure containing either magnesium and aluminium ($MgAl_2Si_4O_{12}$), or lithium ($LiAlSiO_4$: β-eucryptite); small amounts of α-cordierite ($2MgO\text{-}2Al_2O_3\text{–}5SiO_2$) and mullite ($3Al_2O_3\text{–}2SiO_2$) (Fig. 5).

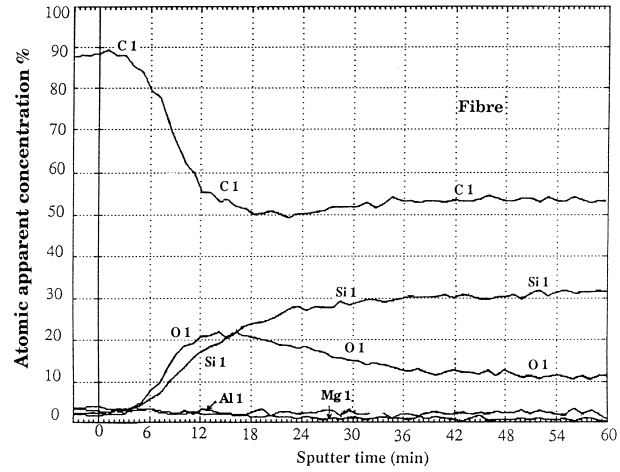

Fig. 2. AES-depth concentration profiles recorded radially from the surface of a pulled-out fibre present at the failure surface of an as-received 0–90° SiC/MAS-L tensile test specimen. The etching rate was 8 nm min^{-1} (standard: Ta_2O_5).

*A BSU is a stack of a few carbon layers of limited lateral size.

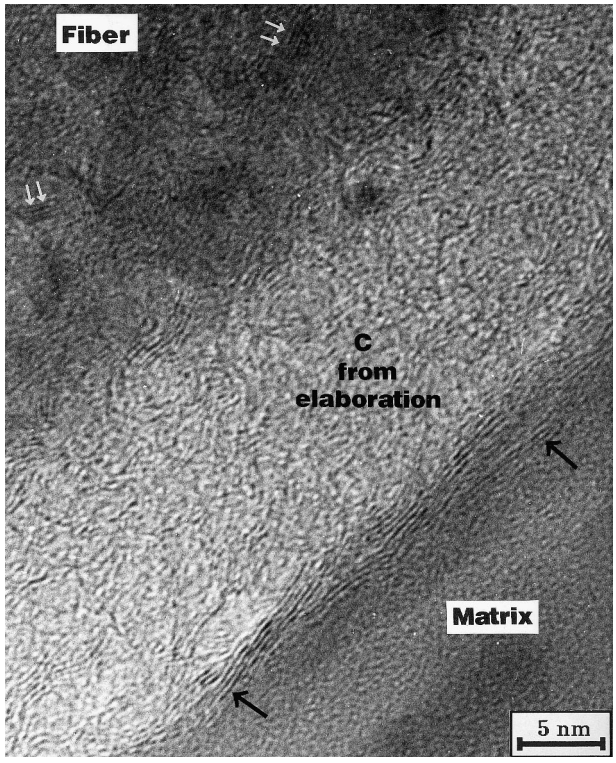

Fig. 3. TEM lattice fringe image of the fibre/matrix interfacial zone in an as-received 0–90° SiC/MAS-L composite. The free carbon BSUs in the fibre are shown with the double arrows.

Pockets of amorphous or partially crystallized phase are located by TEM near the fibres surface, or inside the matrix with a $LiAlSi_2O_6$ chemical composition, as-determined by Monthioux.[19] An intergranular phase with some free carbon is also detected inside the matrix. This phase comes from residues of pyrolysed binding materials used in the preimpregnation process.[19,23] The carbon is spread non homogeneously in the matrix ranging between 1 and 12 at%.

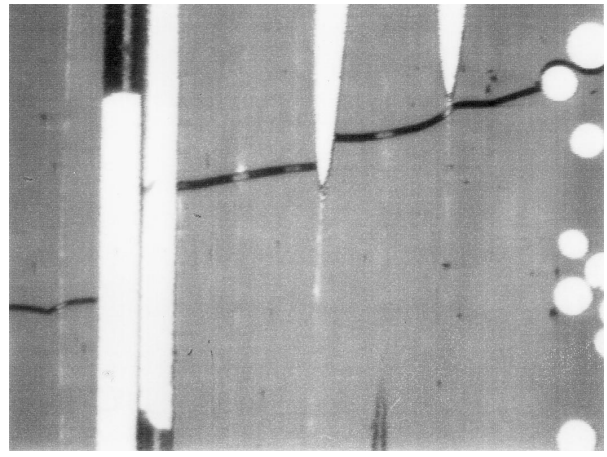

Fig. 4. Optical micrograph of the as-received 0–90° SiC/MAS-L composite: state of damage after tensile test at room temperature.

3.2 Vacuum or argon environment

Ageing treatments under vacuum or under a partial pressure of argon (70 kPa) resulted in a rapid weight loss of the composite as the temperature exceeded 1100°C (Fig. 6) In these conditions, $\Delta m/m_0$ values could reach 20%. These values are very high. They could be linked to the silicated matrix change or to reactions between the fibre and matrix rather than to a change in the fibre which is known to remain stable up to 1000–1100°C.[24] Nevertheless, this matrix is heterogeneous and EPMA analyses found scattered results similar to the as-received composite ones [Table 2(a)]. After ageing, it was not possible to correlate the matrix total composition change to any characteristic chemical phenomenon. It is worthy of note that lithium analyzed by PEELS was detected in some but not all of the tested fibres and matrices of the aged composites [Table 2(a) and (b)].

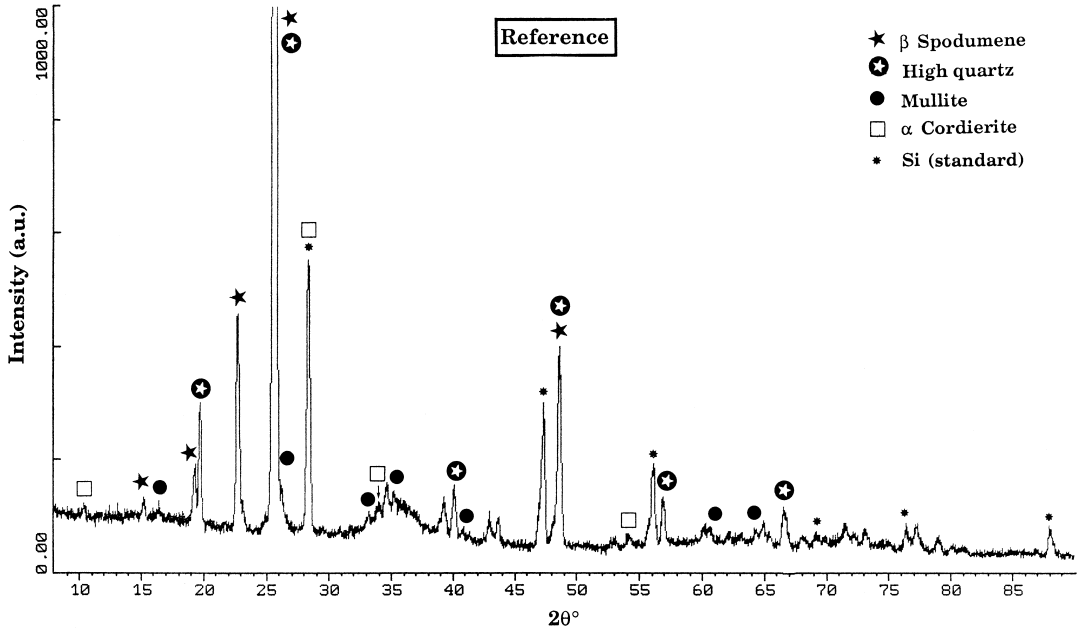

Fig. 5. XRD pattern for the matrix in an as-received 0–90° SiC/MAS-L composite.

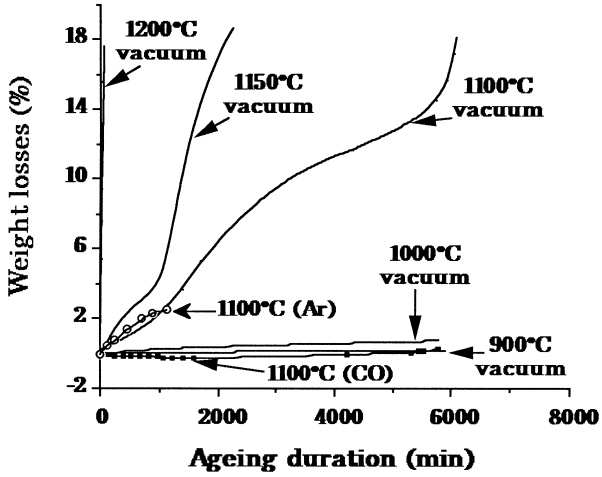

Fig. 6. Weight loss experienced by 0–90° SiC/MAS-L tensile specimens during ageing treatments in the 900–1200°C range, performed under vacuum (residual pressure: 10^{-3} Pa), argon (70 kPa) or *CO* (100 kPa).

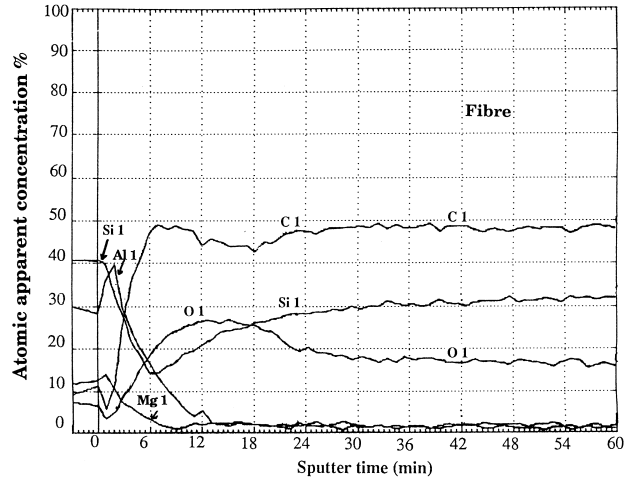

Fig. 7. AES-depth concentration profiles recorded radially from the surface of a pulled-out fibre present at the failure surface of a 0–90° SiC/MAS-L tensile test specimen aged at 1000°C during 96 h under vacuum (residual pressure: $5{\cdot}10^{-4}$ Pa). The etching rate was 8 nm min^{-1} (standard: Ta_2O_5).

3.2.1 T ≤ *1000°C*

Ageing treatments conducted under vacuum during ≈ 100 h at 900 or 1000°C did not cause any changes to the fibres. The fibres still had 2–3 nm SiC-nanocrystals and 100 nm oxygen-rich surface with a bulk chemical composition nearly unchanged [Table 2(b)]. The initial carbon interphase was still 20 nm thick with a microstructure similar to the one described in Section 3.1. Nevertheless, AES depth analyses of a pulled-out fibre at the failure surface of a tensile test specimen aged during 96 h at 1000°C indicated a fibre/matrix decohesion very near the matrix side, and a pronounced diffusion of silicon, Al and Mg (light elements) from the matrix inside the fibre (i.e. 100 nm deep) (Fig. 7) Magnesium concentration was homogeneous in the whole fibre with a value of 0·2 at% slightly superior to the one measured in the as-received composite [Table 2(b)]. SEM micrographs of the failure surface of the 96 h–1000°C aged tensile test specimen showed matrix remaining on the pulled-out fibres (Fig. 8) (not detected in the reference micrograph, Fig. 1). The remaining matrix gave evidence of an increase in the FM bonding intensity, probably explained by the diffusion of Si, Al and Mg elements from the matrix (Fig. 7).

Moreover, the state of crystallization of the matrix differed as soon as the temperature rose above 900°C. After 98 h ageing at 900°C, the main change was a decrease of the β-spodumene phase (Fig. 9) whereas α-cordierite developed in the 96 h–1000°C aged matrix with no more 'high quartz' structure (Fig. 10)

Tensile stress–strain curves recorded for 0–90° SiC/MAS-L composites aged up to 1000°C under vacuum exhibited an ultimate failure stress σ_r higher than in the reference (i.e. 190 versus 170 MPa) (Fig. 11) The maximum strain, ε_r, was also more important (i.e. 0·65% for a 900°C ageing

Table 2. Chemical composition assessed by EPMA in 0–90° SiC/MAS-L composites aged at 1000 and 1100°C under vacuum (residual pressure: 10^{-1}–10^{-3} Pa) or CO (100 kPa): (a) matrix and (b) fibre. Error (at%)≤1

Sample	*Atomic %*					
	Si	*C*	*O*	*Al*	*Mg*	*C/Si*
As-received(**) (a)	18–22	1–12	57–63	8–12	2–3	
Vacuum						
1000°C, 96 h						
1100°C, 16 h(+)	18–22	1–12	57–63	8–12	2–3	
1100°C, 102 h(+)						
CO, 1100°C, 96 h(+)	18–22	1–12	57–63	8–12	2–3	
As-received(**) (b)	37	47	16	–	0·1	1·27
Vacuum						
1000°C, 96 h	37	47	16	–	0·2	1·27
1100°C, 16 h(+)	37	47	16	–	0·1	1·27
1100°C, 102 h(+)	38	46	15·5	–	0·5	1·21
CO, 1100°C, 96 h(+)	34	42	20	3	1·3	1·24

PEELS analysis for Li: (**) present; (+) absent.

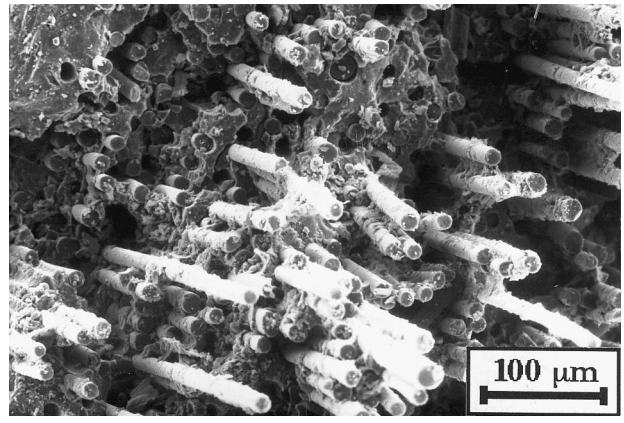

Fig. 8. SEM micrograph of the failure surface of a 0–90° SiC/MAS-L tensile test specimen aged at 1000°C during 96 h under vacuum (residual pressure: $5{\cdot}10^{-4}$ Pa).

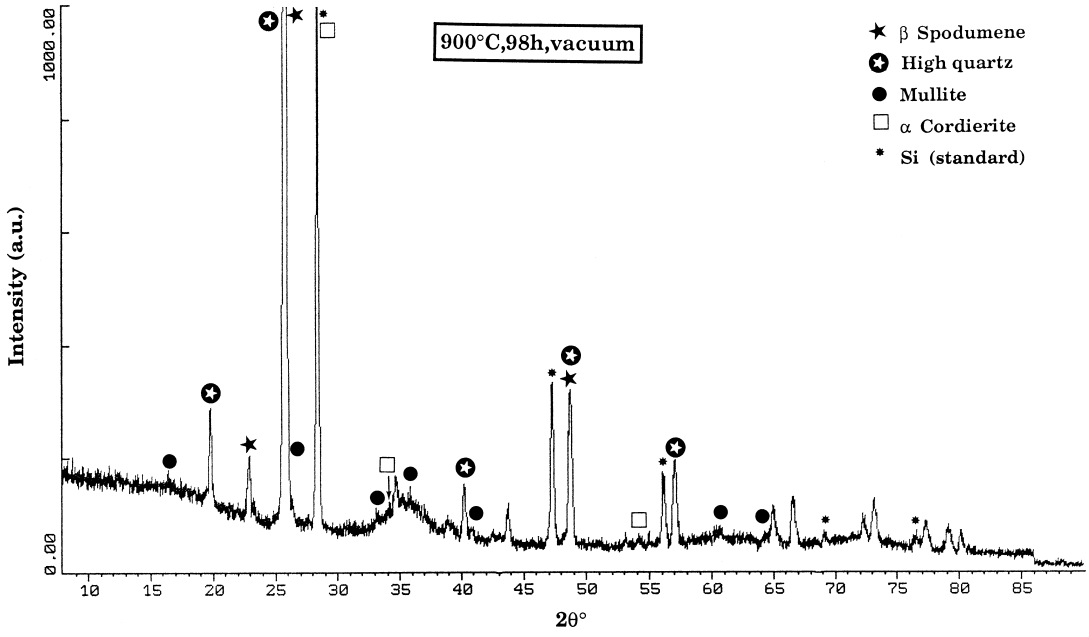

Fig. 9. XRD pattern for the matrix in a 0–90° SiC/MAS-L composite aged at 900°C during 98 h under vacuum (residual pressure: 1·10–3 Pa).

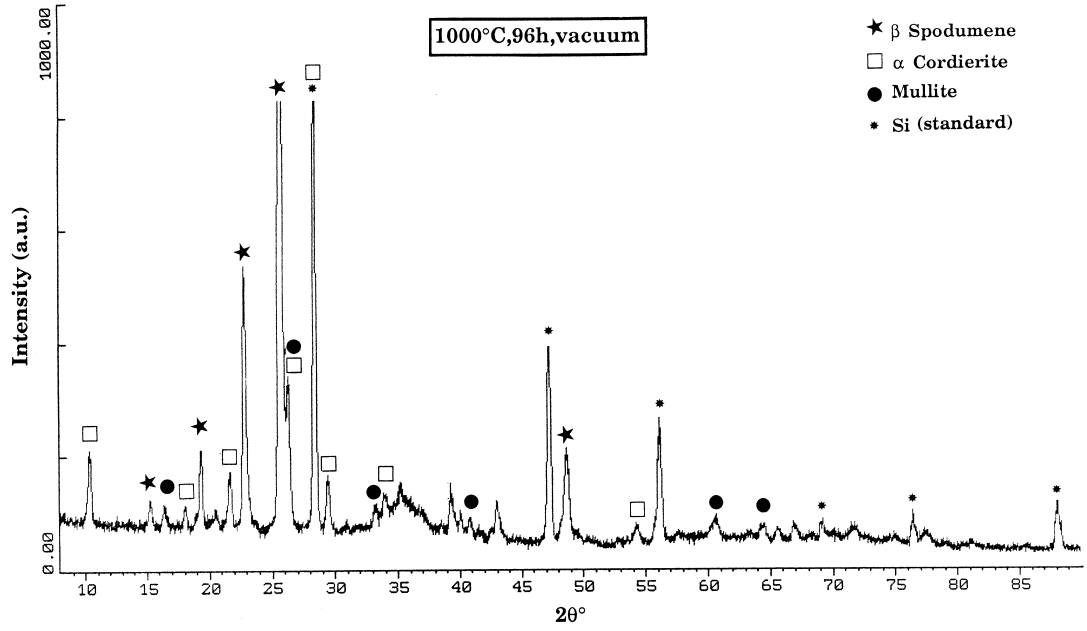

Fig. 10. XRD pattern for the matrix in a 0–90° SiC/MAS-L composite aged at 1000°C during 96 h under vacuum (residual pressure: $5{\cdot}10^{-4}$ Pa).

versus 0·42%) with a fibre pull-out as pronounced as in the reference. Concerning the damage state of the matrix, optical observations showed closed microcracks in the reference, once tensile stress had been relaxed, but open cracks in the 900°C aged specimen with a mean spacing, δ, equal to 200 μm. The latter observation was related to a better ability for the aged composite to transfer load onto the fibres. The Young's modulus decreased more seriously for the specimen aged at 1000°C rather than for the one aged at 900°C, respectively 75 and 87 GPa, revealing thus a greater change in the 1000°C aged composite, as-foreshadowed by the change in the matrix XRD patterns (Figs. 9 and 10).

3.2.2 T = *1100°C*

Ageing treatments at 1100°C under vacuum or argon were 16–100 h long (Table 1). The tensile test specimen aged under vacuum experienced a weight loss of 3% even after 16 h and 12% after 45 h (Fig. 6). After 102 h ageing, external sheets of the aged specimen consisted of fibres without matrix material, as-observed by SEM. The absence of matrix material explained the high weight losses

(i.e. 18·7%). In this case, fibres slightly changed with a *SiC*-crystal growth up to 5–6 nm (TEM analyses) and a bulk chemical composition richer in magnesium (i.e. 0·5 at%) (Fig. 12) Lithium was not detected in the bulk [Table 2(b)]. The carbon interfacial layer formed during the process changed with the ageing time: (i) increased its thickness in the early hours of ageing under vacuum or argon (i.e. $e = 60$ nm for $t < 20$ h) (Fig. 13) and (ii) changed into a layer of large SiC-crystals after 100 h under vacuum (Fig. 14) Moreover, TEM micrograph of the 16 h–1100°C-vacuum aged fibre/matrix interfacial zone revealed the location of the FM decohesion just beneath the 3–4 nm anisotropic carbon border on the matrix side (previously noticed in the reference) (Fig. 13). The AES analyses of the 102 h aged fibre surface confirmed a composition similar to the SiC one with not much oxygen. The matrix began to change as soon as temperature reached 1100°C under vacuum: (i) XRD patterns showed an increase in the α-cordierite and mullite crystallization without β-spodumene or 'high quartz' structure (Fig. 15) and (ii) PEELS analyses did not exhibit any lithium in the bulk [Table 2(a)]. Under a partial pressure of argon, the matrix material did not change as much as under vacuum: (i) β-spodumene phase was still present with no more 'high quartz' structure and (ii) α-cordierite had not crystallized (Fig. 16)

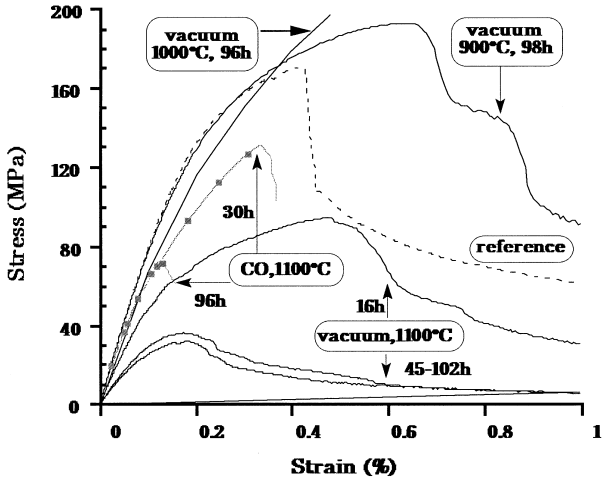

Fig. 11. Tensile stress–strain curves of 0–90° SiC/MAS-L composites tested at room temperature in the as-received state or after ageing treatments performed under vacuum (residual pressure: 10^{-3} Pa) or CO (pressure: 100 kPa).

Tensile curves corresponding to 1100°C vacuum ageing treatments indicated low values for the ultimate failure stress (i.e. $\sigma_r = 94$ MPa for $t = 16$ h, $\sigma_r = 35$ MPa for $45 < t(h) < 102$) (Fig. 11). Moreover, the elastic limit for those specimens was relatively low (i.e. $\sigma_{elast} = 45$ MPa for $t = 16$ h, $\sigma_{elast} = 20$ MPa for $45 < t(h) < 102$). On the other hand, the state of the FM interfacial bonding was assessed by push-out tests (Fig. 17) In such a system with lack of F/M cohesion, the frictional coefficient

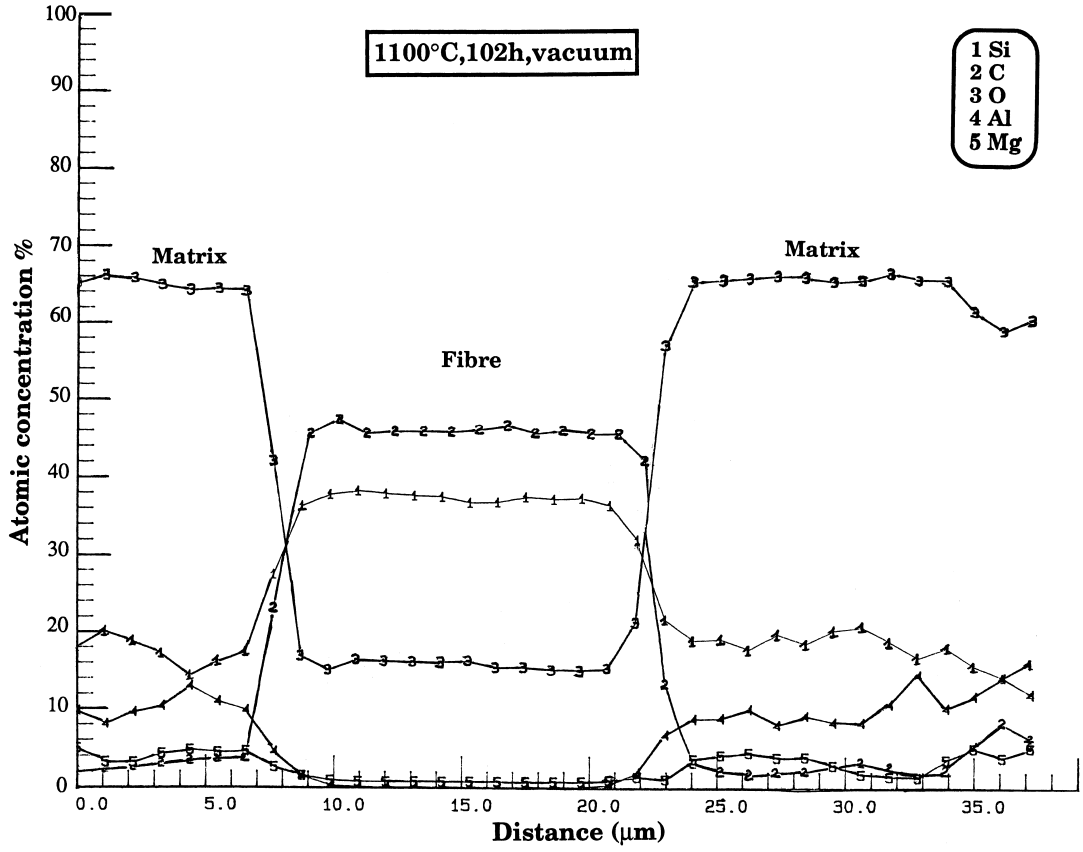

Fig. 12. EPMA radial concentration profiles for a fibre and the surrounding matrix in a 0–90° SiC/MAS-L composite aged at 1100°C during 102 h under vacuum (residual pressure: 10^{-4} Pa). [Si-K(EDS); C-K(WDS); O-K(WDS); Al-K(WDS); Mg-K(WDS)].

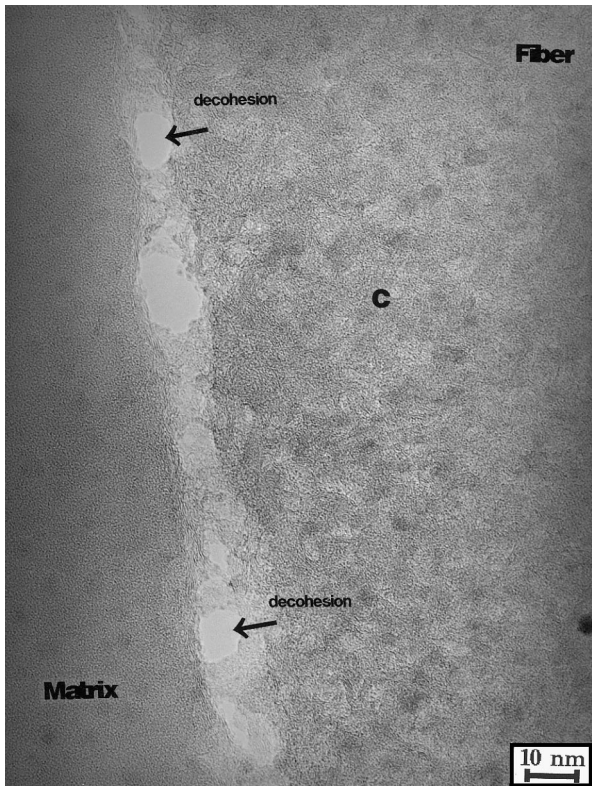

Fig. 13. TEM lattice fringe image of the fibre/matrix interfacial decohesion in a 0–90° SiC/MAS-L composite aged at 1100°C during 16 h under vacuum (residual pressure: $5{\cdot}10^{-3}$ Pa).

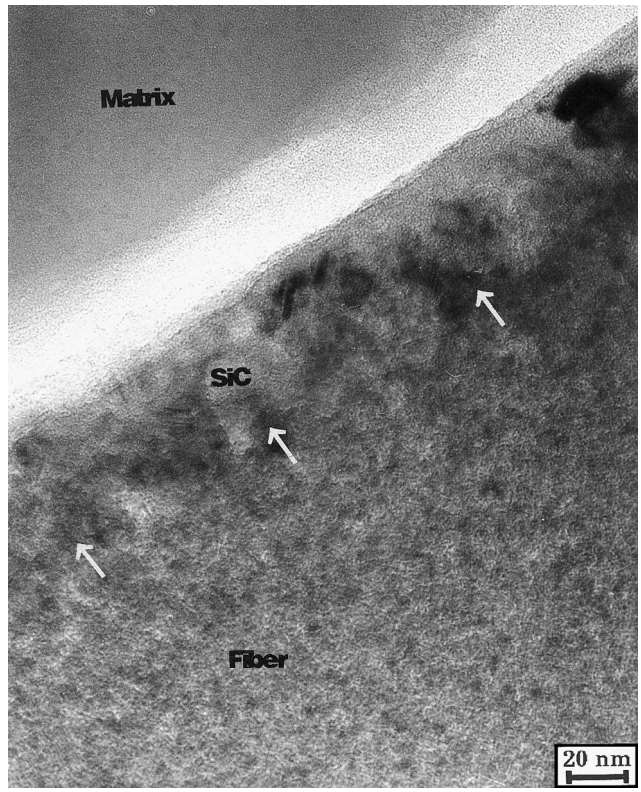

Fig. 14. TEM bright field image of the fibre/matrix interfacial zone in a 0–90° SiC/MAS-L composite aged at 1100°C during 102 h under vacuum (residual pressure: $1{\cdot}10^{-4}$ Pa).

could be considered negligible ($\mu = 0{\cdot}01$)[11] and the model supposing the shear stress τ as having a constant threshold could be applied. Values of τ were thus calculated from the simple relation:

$$\tau = F/2\pi rt \quad \begin{matrix} F : \text{applied load} \\ r : \text{fibre radius} \\ t : \text{foil thickness} \end{matrix} \qquad (1)$$

Push-out curves exhibited quite the same level of critical force (i.e. $F_c = 0{\cdot}05$ N) for the reference, the 96 h–1000°C-vacuum or the 16 h–1100°C-vacuum aged composite. Calculation obtained through 15–30 tests onto 15 μm fibres gave an average value of τ equal to 5 MPa for the reference and the 1000°C aged composite, and to 6 MPa for the 1100°C aged composite (Table 3). The scattering of τ values for the 1000°C aged material was nevertheless much more limited. Our results were similar to Passilly *et al.*[12] which were obtained through push-in on similar composites. Concerning the 45 h–1100°C-vacuum aged composite, matrix degradation was so extreme that it was not possible to prepare any thin foils. Moreover, the TEM observation of the interfacial zone indicated that τ was probably very low (i.e. $\tau <$ 5 MPa). Part of the push-out curves relating to the friction showed by another way a smooth sliding characteristic of composites for which $\alpha_m < \alpha_f$.[25]

3.3 CO environment

Ageing treatments under a CO atmosphere of 100 kPa at 1100°C (Table 1) did not lead to any noticeable weight change even after long ageing times (i.e. $\Delta m/m_0 = \pm 0{\cdot}2\%$) (Fig. 6). Fibres from 30 h–1100°C-CO aged composite exhibited unchanged *SiC*-grain size compared to the reference, whereas those from 96 h–1100°C-CO aged material showed a slight grain growth (i.e. SiC = 5 nm). Their chemical composition was richer in oxygen (i.e. 20 at%), aluminium (i.e. 3 at%) and magnesium (i.e. 1·3 at%) (Fig. 18). C/Si ratio decreased slightly comparative to the reference (i.e. 1·24 versus 1·27) [Table 2(b)]. AES depth profiles measuring the fibre surface chemical compositions also confirmed the results (Fig. 19) Lithium was not detected in the fibres [Table 2(b)]. Fibre/matrix interfacial zone was modified by the appearance of an anisotropic carbon layer which increased with ageing time (i.e. e = 15 nm for t = 30 h, e = 70 nm for t = 96 h) (Figs. 20 and 21). On the other hand, the initial 20 nm carbon layer formed on the fibre surface during elaboration increased threefold after 96 h ageing (Fig. 21) although it had not changed after 30 h ageing (Fig. 20). Matrix of the 1100°C-CO-30 h or 96 h aged composite had a glassy structure more pronounced than in the reference (Figs. 22 and 5) or vacuum-aged sample (Fig. 15). EPMA analysis of the matrix chemical composition did

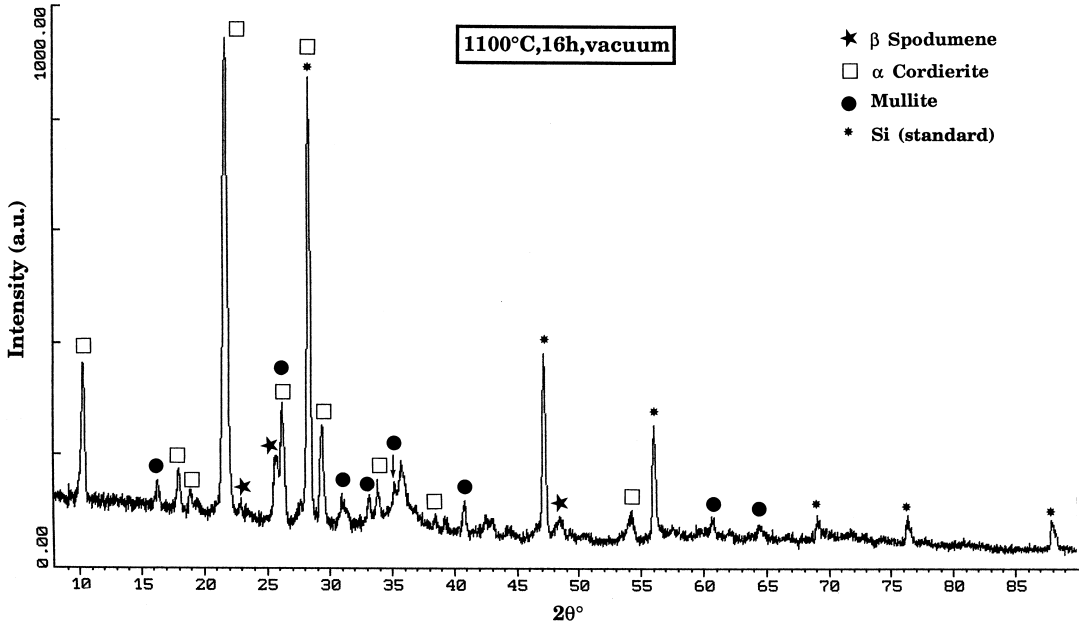

Fig. 15. XRD pattern for the matrix in a 0–90° SiC/MAS-L composite aged at 1100°C during 16 h under vacuum (residual pressure: $5{\cdot}10^{-3}$ Pa).

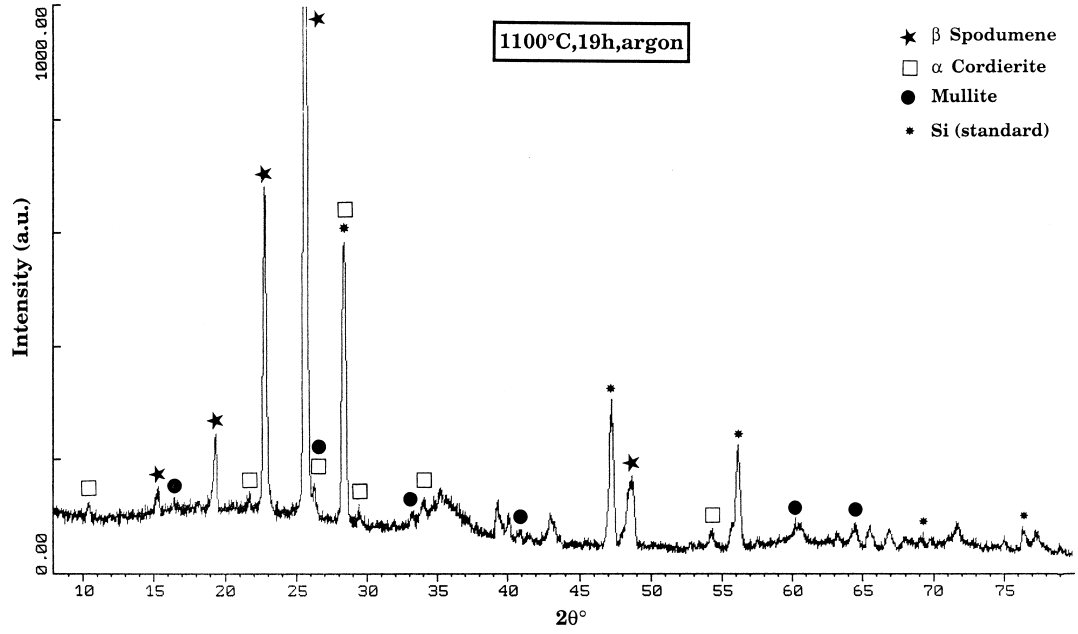

Fig. 16. XRD pattern for the matrix in a 0–90° SiC/MAS-L composite aged at 1100°C during 19 h under argon (pressure: 70 kPa).

not distinguish any fundamental difference from the reference [Table 2(a)]. PEELS analysis revealed that lithium presence in the matrix was at random.

Tensile tests recorded for the 1100°C-CO-96 h aged SiC/MAS-L composites showed that Young's modulus was very near the reference one (i.e. $E = 85$ MPa) (Table 1, Fig. 11). Nevertheless, ageing time has a harmful effect on (i) the ultimate failure stress which decreases from 170 to 130 MPa after 30 h ageing, then to 70 MPa after 96 h ageing and (ii) the failure strain which drops from 0·3 to 0·16% at the same time. Corresponding push-out curves exhibited a level of critical force higher than the reference (Fig. 17). The average value of τ calculated on the basis of equation (R1) was consequently a little higher (i.e. $\tau = 7$ MPa) (Table 3).

4 Discussion

4.1 Physical and chemical aspects

Changes in the matrix are strongly subordinate to temperature (i.e. above 1000°C under vacuum) (Figs. 5 and 10) and the nature of the ageing

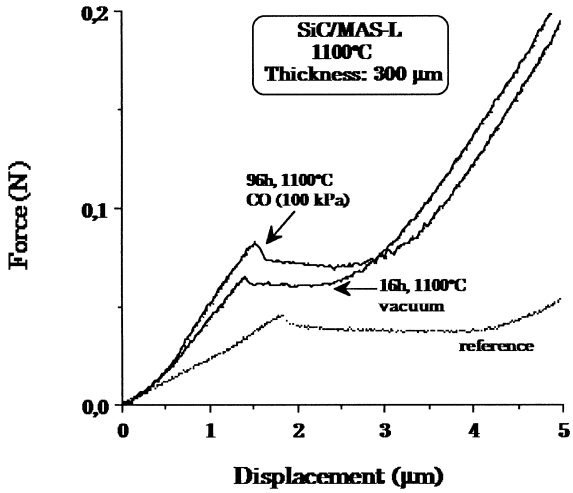

Fig. 17. Representative load-displacement push-out test curves recorded for 0–90° SiC/MAS-L composite thin foils ($t = 300\,\mu$m), in the as-received state or aged under vacuum (residual pressure: $5{\cdot}10^{-3}$ Pa) or a CO atmosphere (100 kPa).

Table 3. Push-out results obtained on aged 0–90° SiC/MAS-L composites. F_c value is an average over 15–30 tests. The diameter of tested fibres is about 15 μm

Sample	*t* (µm)	*Critical F (N)*	*τ (MPa)*
As-received	265	0·05 ± 0·02	5 ± 2
Vacuum			
1000°C, 96 h	235	$0{\cdot}05 \pm 5{\cdot}10^{-3}$	5 ± 0·5
1100°C, 16 h	310	0·08 ± 0·03	6 ± 2
CO (100 kPa)			
1100°C, 96 h	270	0·08 ± 0·02	7 ± 2

atmosphere (Figs. 15,16 and 22). Crystallographic and chemical changes of the matrix material of the aged SiC/MAS-L composites cause a noticeable variation in the thermal expansion coefficient (α matrix = 0·9–1·7 10^{-6} K^{-1} in the initial state, α cordierite = 2·6 10^{-6} K^{-1}, α mullite = 5 10^{-6} K^{-1}). Differences between α_f and α_m after ageing definitely alter F/M bonding.

Under vacuum, the tendency is crystallization of matrix into α-cordierite and mullite as early as 1000°C (Figs. 10 and 15). Argon atmosphere limits the change of the matrix (Fig. 16) whereas CO atmosphere contributes to its vitrification (Fig. 22). Changes can probably be explained by migration of cationic species like Li, Al and Mg from the matrix to the fibre and/or by a selective evaporation of some oxides. It has been shown that the removal of the β-eucryptite phase under a vacuum-1000°C–96 h ageing can be justified either by lithium migration or by Li_2O evaporation, Al and Mg elements being captured respectively in the formation of α-cordierite and mullite. This phenomenon is accelerated with temperature since for short ageing times at 1100°C (i.e. $t = 16$ h) (Fig. 15) it was observed: (i) a complete disappearance of the β-eucryptite as shown previously, (ii) a noticeable decrease of the β-spodumene phase quantity and (iii) a growth of α-cordierite and mullite. Moreover the assumption of Li_2O evaporation seems to be the most probable since no Li was detected in the matrix by PEELS analysis. This kind of evaporation could also explain the fact that, under argon, matrix changes are similar to those recorded under vacuum but much more damped (Fig. 16) (i.e. for a same ageing time) due to the counter-pressure limiting species volatilization (Fig. 6).

Under CO, matrix amorphous regions change with the disappearance of the LAS major phase (Fig. 22) suggesting a reaction between this LAS phase and carbon monoxide.

A glassy structure leading to an increase diffusion rate of Al^{3+} and Mg^{2+} cations could also explain the high quantities of Al and Mg in the fibre (i.e. Al = 3 at%, Mg = 1·3 at%) [Table 2(b)].

Excess of oxygen in the fibres of a 96 h–1100°C-CO aged composite (i.e. O = 20 at%) can be considered as linked to previous cations diffusion. It could thus balance positive charges brought by those cations (i.e. contribution of 3 Al atoms, 1 Mg atom and 6 oxygen atoms versus 2 carbon atoms depletion) [Table 2(b)]. On the other hand, slight SiC-grain growth in the fibre (i.e. 5 nm) and global decrease of its carbon amount justify leaving out a reaction involving CO and the fibre SiC.

Growth of a carbon layer at the fibre/matrix interface during SiC/vitreous ceramic composites elaboration has been widely discussed.[7,26,27] Admitted process is based upon oxidation of fibre silicon carbide by oxidizing matrix:

$$SiC(s)_{(fibre)} + O_2(g) => SiO_2(s) + C(s) \qquad (2)$$

At the F/M interface, carbon born of (R2) reaction has to be in equilibrium with silica which assumes a sufficient pressure of CO to prevent the following (R3) reaction (P(CO) > 0·25 atm = 25 kPa at 1450°C).

$$2C_{(interphase)} + O_2(matrix) => 2CO(g) \qquad (R3)$$

Development of the carbon interphase could thus be generated by a diffusion of *CO* through the carbon layer reacting with the surface fibre as following:[27]

$$2CO(g) + SiC_{(fibre)} => SiO_2(s) + 3C(s) \qquad (R4)$$

Nature of the F/M interfacial layers recorded in the as-received SiC/MAS-L composite is (i) a 20 nm bad-organized carbon layer then (ii) an oxygen-rich layer over 100–150 nm on the fibre surface (Figs. 2 and 3). Those results confirm oxidation of the fibre surface by species coming from the matrix (R2,R3,R4 reactions).

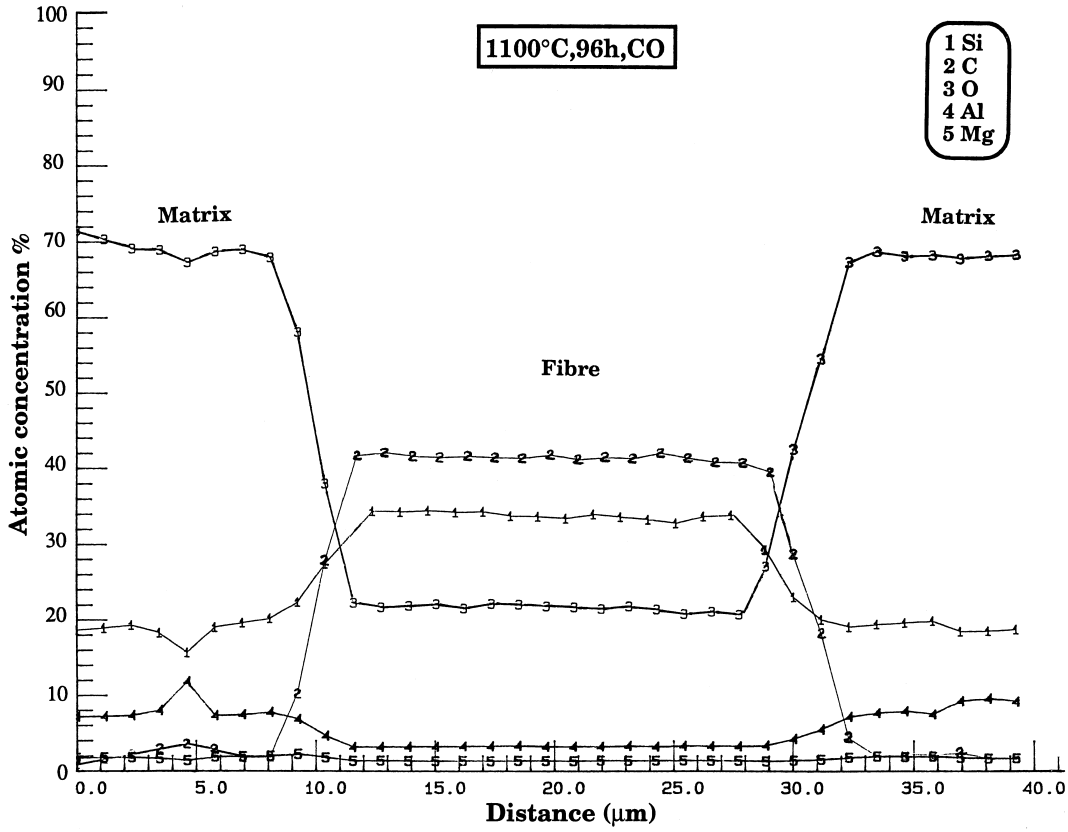

Fig. 18. EPMA radial concentration profiles for a fibre and the surrounding matrix in a 0–90° SiC/MAS-L composite aged at 1100°C during 96 h under CO (100 kPa). [Si-K(EDS); C-K(WDS); O-K(WDS); Al-K(WDS); Mg-K(WDS)].

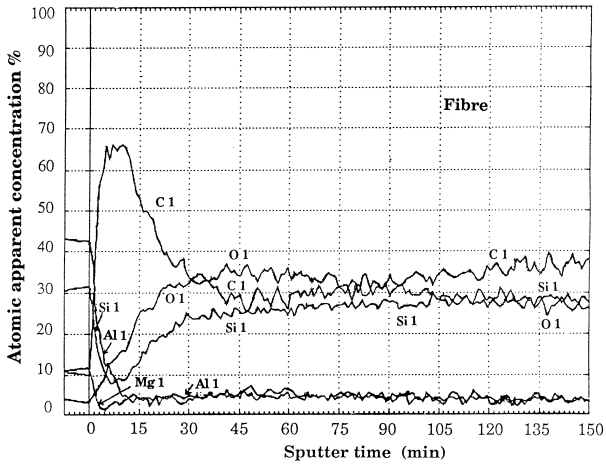

Fig. 19. AES-depth concentration profiles recorded radially from the surface of a pulled-out fibre present at the failure surface of a 0–90° SiC/MAS-L tensile test specimen aged at 1100°C during 96 h under CO (100 kPa). The etching rate was 8 nm min^{-1} (standard: Ta_2O_5).

Ageing treatments achieved at temperatures lower than the elaboration one (i.e. 900 and 1000°C during 100 h under vacuum) promote the diffusion of Si, Al and Mg from the matrix to the fibre (Fig. 7) without altering the structural state of the 20 nm initial interfacial carbon layer. However, Al is still concentrated in the extreme surface (possibly fixed into the aluminosilicates) whereas Mg spreads into the whole bulk of the fibre in small concentration, even after 96 h at 1100°C (i.e. 0·2 at%) [Table 2(b)]. As soon as temperature reaches 1100°C under vacuum, the F/M interfacial zone changes into two steps: (i) a growth of the interfacial carbon (i.e. $e = 60$ nm for $t = 16$ h) (Fig. 13) then (ii) for longer times, a change of the carbon interphase as well as the fibre surface into SiC, coupled to a decrease of the oxygen amount. Whatever the ageing time, the chemical composition of the fibre in the bulk does not change [Table 2(b)]. The first step can be explained through the R2, R3 and R4 reactions. The second one can probably be justified by $SiO(g)$ emission coming from the matrix and/or the fibre extreme surface, reacting thus with the carbon interfacial zone in the following manner:

$$2C_{(\text{interphase})} + SiO(g) \Rightarrow SiC(s) + CO(g) \quad (R5)$$

Under CO at 1100°C, the interfacial zone changes through the appearance of an anisotropic carbon layer on the matrix side increasing with the ageing time (i.e. $e = 15, 70$ nm for $t = 30, 96$ h), which may be linked to the amorphization of the matrix under such an atmosphere. Diffusion of the fibre free carbon [Table 2(b)] could explain the increasing carbon layer (made of BSU in turbostratic disorder) on the fibre surface after 96 h ageing (Fig. 21).

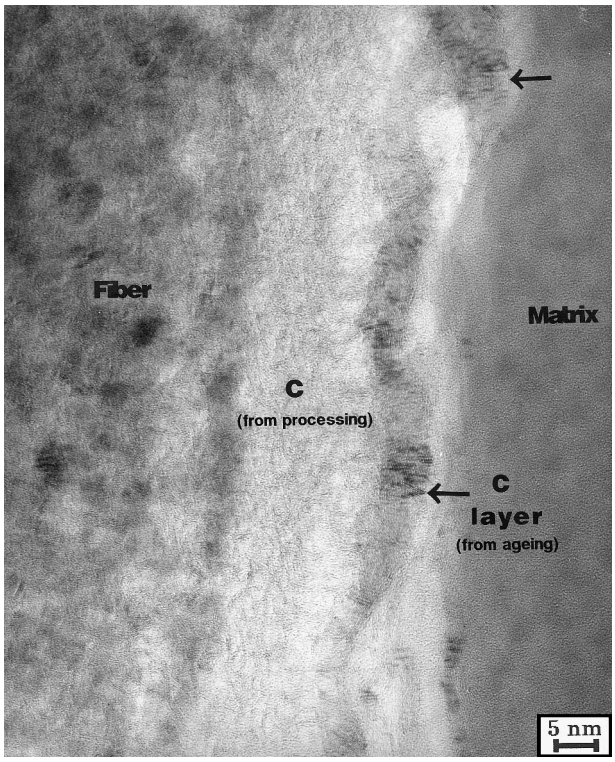

Fig. 20. TEM lattice fringe image of the fibre/matrix interfacial zone in a 0–90° SiC/MAS-L composite aged at 1100°C during 30 h under CO (100 kPa).

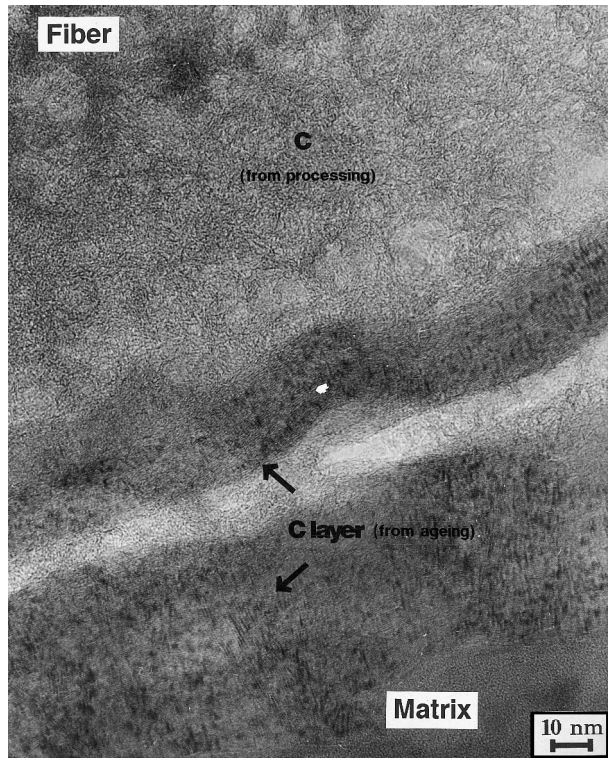

Fig. 21. TEM lattice fringe image of the fibre/matrix interfacial zone in a 0–90° SiC/MAS-L composite aged at 1100°C during 96 h under CO (100 kPa).

4.2 Mechanical aspects

Tensile tests at room temperature as well as push-out tests gave the change in the mechanical behaviour of the aged SiC-MAS-L composites (Figs. 11 and 17 and Table 3).

Tensile curves can be divided into two groups: (1) those which give some values of failure strain and stress higher than the reference ones with a similar Young's modulus and (2) those for which the Young's modulus is widely lower than the reference with low failure strain and stress. Group (1) corresponds to materials in which fibres are kept unchanged, matrix has only slightly developed and the interfacial zone contains migrating elements from the matrix to the fibre (i. e. Si, Al and Mg at 900 and 1000°C under vacuum) (Fig. 7). This interfacial evolution is profitable to transfer the load between fibres and matrix since the level of failure stress has increased from 170 to about 195 MPa with a slight increase of the failure stress (i.e. higher than 0·42%). The interfacial bonding is uniform in the 96 h–1000°C-vacuum aged composite since the scattering for the τ values is low (i.e. $\tau = 5 \pm 0{\cdot}5$ MPa versus $\tau = 5 \pm 2$ MPa in the reference) (Table 3). This tends to confirm a higher strength in the F/M bonding after long treatments at 1000°C under vacuum. The lowest values of τ from the reference (i.e. 3 MPa) are probably due to a lack of bonding between the fibre and matrix. Nevertheless, the untimely failure of the corresponding tensile-test specimen (Fig. 11) can be explained by an advance matrix change with (i) beginning of the crystallization into α-cordierite and mullite and, (ii) disappearance of β-eucryptite (Fig. 10), leading to a decrease in the composite Young's modulus (i.e. 75 versus 93 GPa). Ageing treatments at 1100°C under vacuum reveal the fatal consequence of the matrix crystallization. They do lead to tensile curves of group (2) (Fig. 11). Young's modulus gets lower and lower with increasing crystallization (i.e. E = 59 GPa after 16 h under vacuum and E = 35 GPa after 45 h), which might be explained by a matrix cracking during cooling of the tensile-test specimen (Fig. 15). The F/M bonding in those composites was characterized by an interfacial shear stress similar to the reference one (i.e. $\tau = 5$–7 MPa) (Fig. 17) which can not justify the difference recorded between the tensile curves (Fig. 11). On the other hand, the very low mechanical characteristics of the $t > 50$ h–1100°C-vacuum aged material can also partly be explained by a weakening of the F/M bonding which becomes non-existing after the SiC-grain growth at the fibre surface.

Ageing treatments under CO changed both the F/M interfacial zone, matrix structure and fibres chemical composition [Figs. 20–22, Table 2(b)]. The matrix appears vitreous contrary to vacuum treatments (Figs. 15 and 22) which might lead to a higher value of the Young's modulus (i.e. $E = 85$ GPa until 96 h under *CO* versus $E = 59$ GPa after 16 h under

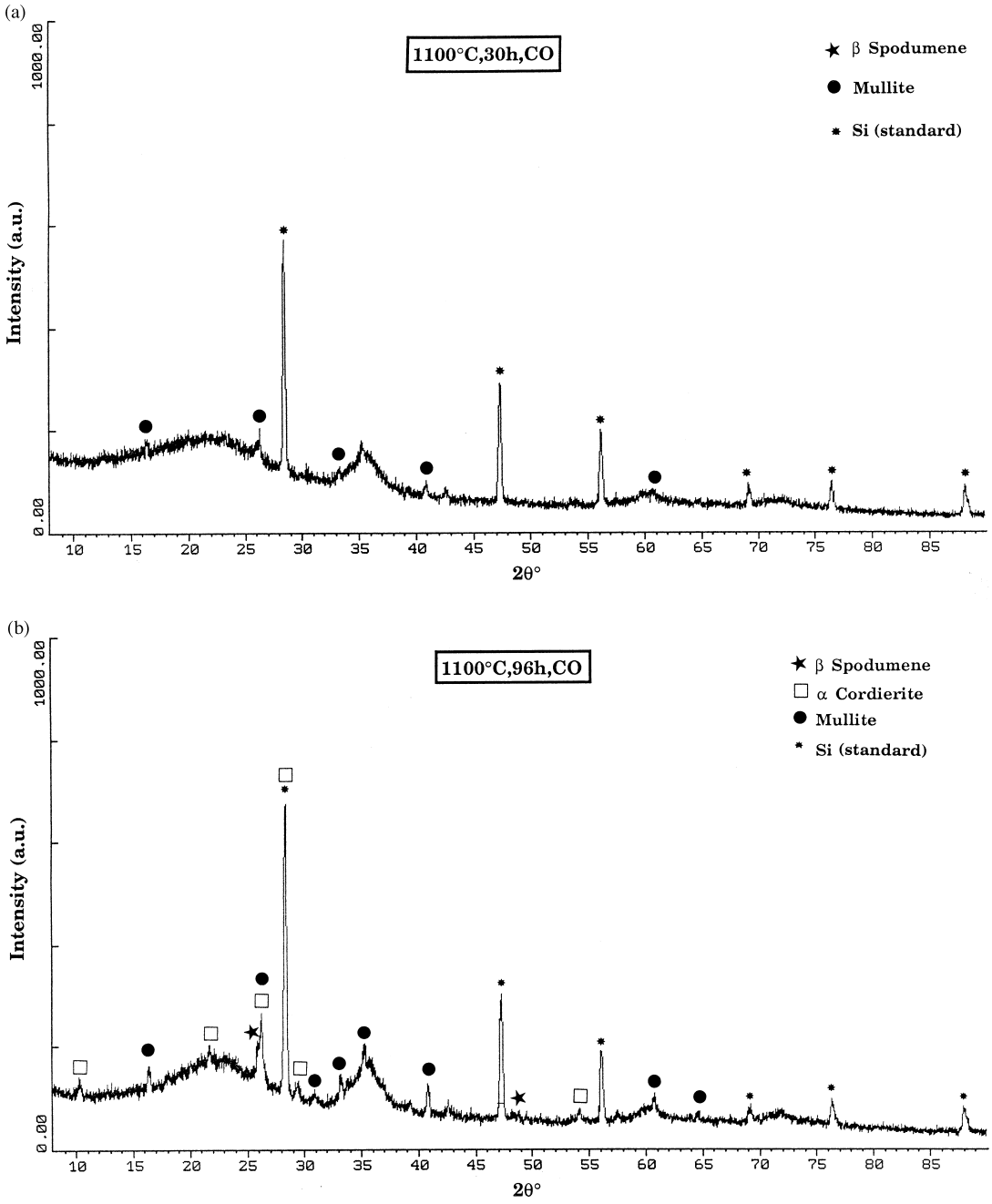

Fig. 22. XRD pattern for the matrix in a 0–90° SiC/MAS-L composite aged at 1100°C under CO (100 kPa): (a) 30 h and (b) 96 h.

vacuum). Enrichment of fibres into migrating species coming from the matrix, between 30 and 96 h ageing, can probably explain the advance failure of the tensile-test specimen at $\varepsilon = 0{\cdot}16\%$ versus 0·33% [Fig. 11, Table 2(b)]. The interfacial zone is characterized by the simultaneous growth of the initial carbon interphase on the fibre side and of an anisotropic carbon layer on the matrix side. In this case, the value of the interfacial shear stress is slightly higher than in the reference sample or the vacuum-aged composite samples (i.e. $\tau = 7 \pm 2$ MPa versus 5 ± 2 MPa) (Fig. 17 and Table 3). Thus, the push-out test confirms that the F/M bonding is reinforced (i) by the anisotropic interfacial carbon resulting from reactions with CO (the F/M adhesion is restored and diffusion of elements from the matrix more pronounced) and (ii) by the possible tightening effect of the matrix onto the fibre after change of the matrix thermal expansion coefficient.

5 Conclusion

Changes in the mechanical behaviour of SiC (ex-PCS)/MAS-L composites aged between 900 and 1200°C under controlled atmosphere have been correlated to the structural changes of the matrix, interface F/M zone and fibre.

The MAS-L vitreous ceramic is modified as early as 900°C under vacuum with a proportion of hexagonal 'high quartz' eucryptite phase higher than the β-spodumene phase. As soon as temperature raises above 1000°C, the MAS-L quickly crystallizes into α-cordierite and mullite. This crystallization is harmful to the mechanical behaviour of the material since the Young's modulus rapidly drops at 1100°C ($E = 93$, 59 and 35 GPa respectively for the reference, 16 and 45 h ageing).

Disappearance of LAS phases is less important under an argon atmosphere (i.e. only β-eucryptite vanishes) and does not cause the recrystallization of matrix into α-cordierite and mullite. Changes are probably explained by a migration of Al and Mg cationic species from the matrix to the fibre and by a selective evaporation of some oxides (i.e. Li_2O).

Under a CO atmosphere, tendency is to get an amorphous MAS-L after reactions with the carbon monoxide leading also to a significant diffusion of Al and Mg from the matrix to the fibre.

The chemical composition of SiC (ex-PCS) fibres is not affected by ageing up to 1100°C under vacuum or argon. Nevertheless those treatments modify the fibre/matrix interfacial zone which presents a diffusion of Si, Al and Mg elements coming from the matrix. This migration tends to strengthen the initial weak fibre/matrix bonding and contribute to improve the mechanical properties of the composite ($\sigma_r = 195$ versus 170 MPa and $\varepsilon_r = 0{\cdot}65\%$ versus $0{\cdot}42\%$) as long as the matrix becomes not too much crystallized (i.e. $T \leq$ 1000°C). Under CO, special reactions occur between the atmosphere and matrix inducing the formation at the F/M interface of an anisotropic carbon layer increasing with ageing time. In this case, intensity of the F/M bonding determined by push-out test is stronger than in aged composites in which diffusion phenomena only take place between the matrix and fibre (i.e. average value of $\tau = 7$ versus 5 MPa).

Acknowledgements

This work has been performed within the framework of the national cooperative research program 'Thermomechanical Behavior of Ceramic Matrix Composites' (GS-4C) supported by CNES, DRET, MRES, Aerospatiale, SEP and SNECMA. The authors are indebted to B. Humez (LCTS) for his contribution to the mechanical tests, M. Lahaye and M. Chambon (CUMEMSE, Univ. Bordeaux) for their assistance in the AES and TEM analyses, and X. Bourrat (LCTS) for his contribution to the PEELS analysis. They acknowledge the assistance that they received from Aerospatiale through the supply of the samples and valuable discussions with G. Larnac and P. Pérès.

References

1. Bischoff, E. and Sbaizero, O., The influence of heat treatment on the fibre/matrix interface in a SiC reinforced glass ceramic. *Electron Micros. Soc*., 1988, 46th meeting, 742–743.
2. Bischoff, E., Ruhle, M., Sbaizero, O. and Evans, A. G., Microstructural studies of the interfacial zone of a SiC fiber/reinforced lithium-aluminum silicate glass ceramic. *J. Am. Ceram. Soc*., 1989, **72**(5), 741–745.
3. Brennan, J. J., *Interfacial Characterization of Glass and Glass–Ceramic* Matrix/Nicalon SiC Composites, ed R. E. Tressler, G. L. Messing, C. G. Pantano and R. E. Newnham. Plenum Press, New York, 1986, 549.
4. Brennan, J. J., Interfacial chemistry and bonding in fiber reinforced glass and glass-ceramic matrix composites. *Mat. Sci. Res*., 1986, **21**, 387–399.
5. Brennan, J. J., Interfacial characteristics of glass-ceramic matrix-SiC fiber composites. *J. de Physique*, 1988, **49**(10), 791.
6. Chaim, R. and Heuer, A. H., The interface between (Nicalon) SiC fibers and a glass-ceramic matrix. *Adv. Ceram. Mater*., 1987, **2**(2), 154–158.
7. Cooper, R. F. and Chyung, K., Structure and chemistry of fibre-matrix interfaces in silicon carbide fibre-reinforced glass-ceramic composites: an electron microscopy study. *J. of Mater. Sci*., 1987, **22**, 3148–3160.
8. Mazerolles, L., Michel, D., Ulmer, L., Pastol, J.L., Parlier, M. and Ritti, M. H., Interfaces in SiC fiber-reinforced glass-ceramic composites. *Colloque de Physique C1*, 1990, **51**, 879–883.
9. Marshall, D. B., An indentation method for measuring matrix-fibre frictional stresses in ceramic composites. *J. Am. Ceram. Soc*., 1984, **67**(12), 259–260.
10. Marshall, D. B. and Oliver, W. C., Measurement of interfacial mechanical properties in fibre-reinforced ceramic composites. *J. Am. Ceram. Soc*., 1987, **70**(8), 542–548.
11. Pérès, P., Analyse théorique et expérimentale du rôle des paramètres de microstructure sur le comportement des composites à matrice fragile. thèse de doctorat, INSA de Lyon no. 88, 1988.
12. Passilly, B., Sudre, O. and Parlier, M., Caractérisation mécanique des interfaces dans des composites céramique-céramique. Revue des composites et des matériaux avancés, ed. J. L. Chermant et G. Fantozzi, Hermès, 1993, pp. 253–265.
13. Weihs, T. P. and Nix, W. D., Experimental examination of the push-down technique for measuring the sliding resistance of silicon carbide fibers in a ceramic matrix. *J. Am. Ceram. Soc*., 1991, **74**(3), 524–534.
14. Weihs, T. P., Sbaizero, O., Luh, E. Y. and Nix, W. D., Correlating the mechanical properties of a continuous fiber-reinforced ceramic-matrix composite to the sliding resistance of the fibers. *J. Amer. Ceram. Soc*., 1991, **74**(3), 535–540.
15. Mandell, J. F., Grande, D. H. and Jacobs, J., Tensile behavior of glass/ceramic composite materials at elevated temperatures. *J. of Eng. for Gas Turbines and Power*, 1987, **109**, 267–273.
16. Thouless, M. D., Sbaizero, O., Bischoff, E. and Luh, E. Y., The influence of heat treatment upon fiber pull-out in a ceramic composite. *Mat. Res. Soc. Symp. Proc*., 1988, **120**, 333–339.
17. Larnac, G., Elaboration d'une matrice pour composites céramique-céramique par la voie Sol-Gel. thèse no. 67, Université Montpellier 2, 1990
18. Larnac, G., Pérès, P., Donzac, J. M., Elaboration et caractérisation du composite à matrice vitrocéramique SiC/

MAS-L. *Revue des composites et des matériaux avancés*, Vol. 3, ed. J. L. Chermant et G. Fantozzi, Hermès, 1993, pp. 27–41.
19. Monthioux, M. Nano et microtextures de composites SiC/LAS-M. *Revue des composites et des matériaux avancés,* Vol. 3. ed. J. L. Chermant et G. Fantozzi, Hermès, 1993, 69–90.
20. Cutard, T., Fargeot, D., Gault, C. and Huger, M., Caractérisation par ultrasons à haute température de composites céramique-céramique. *Revue des composites et des matériaux avancés*, Vol. 3, ed. J. L. Chermant et G. Fantozzi, 1993, pp. 113–128.
21. Villeneuve, J. F., Etude de la dilatation thermique et du comportement thermomécanique en traction et en torsion de quelques fibres céramiques monofilamentaires. thèse no. 661, Université Bordeaux I (1991).
22. Grenier, T., Parlier, M. and Passilly, B., In *Interfacial Phenomena in Composite Materials* ed. I. Verpoest et F. Jones, Butterworth-Heinemann Ltd, Belgium, 1991, p. 200.
23. Kervadec, D., Chermant, J. L., Fluage et microstructure du SiC-MLAS 1D. *Revue des composites et des matériaux avancés*, Vol. 3, ed. J. L. Chermant et G. Fantozzi, Hermès, 1993, pp. 173–189.
24. Clark, T. J. and Arons, R. M., Thermal degradation of Nicalon SiC fibers. *Ceram. Eng. and Sci. Proc.*, 1985, **6**(7–8), 576–588.
25. Jero, P. D. and Kerans, R. J., Effect of interfacial roughness on the frictional stress measured using pushout tests. *J. Amer. Ceram. Soc.*, 1991, **74**(11), 2793–2801.
26. Bonney, L. A. and Cooper, R. F., Reaction-layer interfaces in SiC-fiber-reinforced glass ceramics: a high resolution scanning transmission electron microscopy analysis. *J. Am. Ceram. Soc.*, 1990, **73**(10), 2916–2921.
27. Benson, P. M., Spear, K. E. and Pantano, C. G., Interfacial characterization of glass matrix/Nicalon SiC fiber composites: a thermodynamic approach. *Ceram. Eng. Sci. Proc.*, 1988, **9**(7–8), 663–670.